Atmospheric Corrosion Behavior on Low Alloy Steels under Seashore Environment

Kazuhiko Noda, Masahiro Yamamoto*, Hiroyuki Masuda, and Toshiaki Kodama

National Institute for Materials Science (NIMS)
1-2-1 Sengen, Tsukuba 305-0047 JAPAN
*Steel Research Laboratories, Nippon Steel Corporation
20-1 Shintomi, Futtsu 293-8511 JAPAN

Atomic force microscope (AFM) measurements and scanning chemical microscopy (SCHEM) were performed for the investigation of atmospheric corrosion behavior of low alloy steels. The high sensitivity profile was determined by AFM for iron surface with droplets of synthetic seawater following the exposure to corrosive atmosphere. Simultaneously with AFM surface potential on iron was detected using a Kelvin force microscope (KFM) system during rusting process. Microvisualization of rusting iron surface is to be demonstrated in this paper in the form of parallel mapping of profile and surface potential distribution using the in-situ measuring technique. At relative humidity (RH) of 40%, growth rate of rusting on iron greatly increased in comparison with the case of RH of 30%. The water condensation in the presence of $MgCl_2$ is the main reason of the enhanced corrosion rate with increasing of relative humidity. In advance to the rust formation, a zone of less noble potential was detected by KFM around the droplet of synthetic seawater although AFM showed no irregularity in the profile image. It can be explained by this less noble potential that the rusting reaction initiated in the vicinity of the seawater droplet. The efficiency of alloy elements (Ni, Cr) on the atmospheric corrosion morphology was explained by SCHEM system. It has been proven that AFM system combined with KFM and SCHEM system was effective in the investigation of atmospheric corrosion of iron and steel which otherwise was difficult to evaluate by conventional method.

Keywords : *Low alloy steel, atmospheric corrosion, atomic force microscope (AFM), rusting process, scanning chemical microscope (SCHEM)*

1. Introduction

In atmospheric corrosion study of iron and steels, it is difficult to evaluate the corrosion behavior, because the conventional electrochemical method can not be applied to the study. Recently, as the observation of the atmospheric corrosion surface, a few new techniques has been applied in order to understand the behavior. It has been also found out that the potential can be determined by the non-contact Kelvin probe method.[1-11] We also reported the potential distribution of the rusting process on pure iron.[12] One of the authors has also observed the topography and the potential distribution of the droplet which contact to the surface of the metal by AFM.[13] Atomic force microscopy (AFM) measurements were performed for the investigation of rusting process. The high sensitivity profile was determined by AFM for iron surface with the droplet of artificial seawater following the exposure to corrosive atmosphere. Simultaneously with the

surface shape, surface potential on iron was detected using a Kelvin force microscope (KFM) system during rusting process. When the atmospheric corrosion process of the steel material is examined, we must examine an environmental condition in the same way as the characteristic of the material. The pH is also one of the essential factor which controls corrosion behavior as an environmental parameter. Some technique has been tried to measure the surface pH distribution.[14-17]

In this report, the rusting process of the artificial sea salt adherence iron and low alloy steel (Fe-Cr, Fe-Ni steel) was observed, and the potential distribution on the surface rusting was examined to investigate the Cr and Ni additive effect on the atmospheric corrosion in the seashore environment. The pH gradation on the surface in the atmospheric corrosion process of low alloy sheets was determined by using the scanning chemical microscope (SCHEM), and the effect of additive element on localized function was evaluated by this result.

Fig. 1. Schematic diagram of Atomic force microscopy(AFM) and Kelvin force Microscopy(KFM).

2. Experimental

2.1 Observation of corrosion behavior on low alloy steels using AFM/KFM

The experiment was done on pure iron and ferritic alloys (Fe-3mass%Cr, Fe-3mass%Ni steel) used as the test samples and after buff grinding was done on the surface of the samples. A droplet of artificial sea was attached on the sample. After that, the sample was held in the room-temperature and the rust growth process was observed in the fixed relative humidity. The optical microscope and atomic force microscope (AFM) were used for the observation of rusting process on the iron and ferritic alloys under the atmospheric corrosion condition. The rust growing process on the iron and ferritic alloys after wet/drying corrosion cycle test and the surface morphology after elimination the rust film was also observed by the optical microscope.

Nano Scope IIIa of the Digital Instruments company was used for the AFM observation. As for the measurement of only the topography, the Si probe with the resonance frequency of 25kHz was used. Conductive probe with Si prove coated by Au was used for the potential measurement using Kelvin force microscope (KFM). The schematic diagram of the shape observation and the potential distribution measurement on the surface is shown in Fig. 1. Without making the condition on the surface and a form change, and a surface profile could be measured using the non contact (tapping) mode of AFM. Electric potential on the surface was determined rapidly with the surface profile in the high precision by the interleave combination measurement. Potential indication

was shown as a relative potential to know relative potential difference.

2.2 Localized pH measurement

The low alloy steels (Fe-3mass%Cr, Fe-3mass%Ni steel) was also used as the test samples to investigate the localized pH under atmospheric corrosion environment. Corrosion cycle test was also carried out to investigate the corrosion morphology on low alloy steels. After tests, the rust layer was removed from the surface, the observation of the surface roughness was occurred. In pH measurement, 0.1M KCl was added in the agar as an electrolyte, and the process of the corrosion by chloride ion and the moisture in this agar was chased as a surface pH distribution. The pH measuring area was 15 mm x 15 mm on samples and in every 30 minutes the surface pH distribution was measured by scanning chemical microscope.

Scanning chemical microscope (SCHEM-100) on the marketing (HORIBA Co. Ltd.) was used for the surface pH distribution measurement. Schematic diagram of the pH measurement by SCHEM is shown in the Fig. 2. It contacts a sample with the sensor for the pH measurement which semi-conductor and insulator is spread in and which is put together through the agar as an electrolyte, and laser light is irradiated on the surface of the sensor. Sensitizing electric current (photocurrent) due to the optical irradiation flows as a character of the semi-conductor part in the laser irradiation part. Detection can do that laser light is squeezed only the local electric current value by squeezing laser light. Relations between the bias voltage/photocurrent and the pH come to show it in the Fig. 3. Therefore, pH
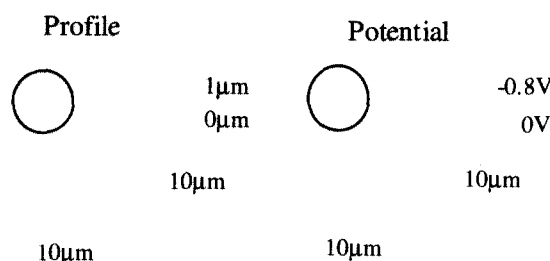
Profile   Potential

1μm   -0.8V
0μm   0V

10μm   10μm

10μm   10μm

after 3 hours
25C 40%RH

Fig. 2. Schematic diagram of SCHEM for pH distribution measurement.

Profile   Potential

1μm   -0.8V
0μm   0V

10μm   10μm

10μm   10μm

Fig. 4. Surface profile and surface potential distribution of rusting process of iron after droping artificial sea water.
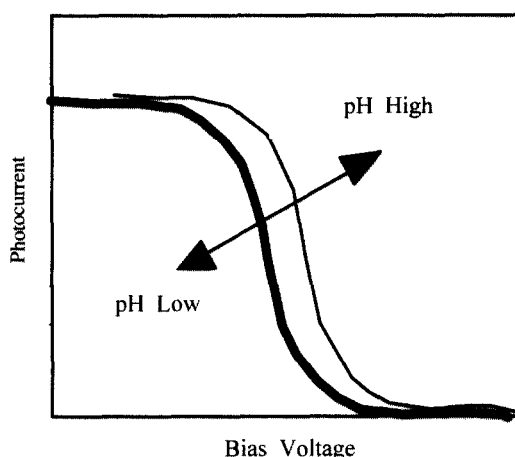
pH High

pH Low

Bias Voltage

Fig. 3. Relations between the bias voltage/photocurrent and the pH value.

on the surface of the sample can be decided by determining the relations of voltage-electric current. Two-dimensional pH measurement can be done by scanning laser light, and then a pH map on the surface of the sample can be prepared.

3. Results and discussion

3.1 The potential distribution of the low ally steels under rhe rust formationt

Artificial sea water of 1μm dropped on pure iron, and it was held at 30%RH for 48 hours. After that, the relative humidity was made 40%RH, and the result which determined a profile on the surface and potential distribution by AFM is shown in Fig. 4. Therefore, the rust was formed by the high concentration solution, because $MgCl_2$ in the artificial sea water becomes a liquid condition. Though the crystallization of NaCl in droplet was seen, rust formation in the low humidity was due to the
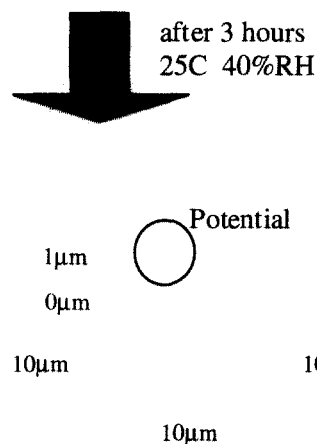
deliquescence of $MgCl_2$ in the artificial sea water. The $MgCl_2$ solution used for the research of the atmospheric corrosion characteristic of the iron at the low humidity was effective. The morphology of rust in the low humidity condition was filiform as seen in Fig. 4.

The rust was formed in the filiform shape and had the height of about 2μm, and this was the size which could not be seen by the macro level rust observation. The rust shape was the micro form of the rust layer which it was commonly aware of as a point rust about this form. This result about filiform shape rust could be thought existence of corrosion products on the surface and the iron dissolution promotion of the tip of the rust and the cathode behavior promotion of the side to be a cause. As for the detail, the water absorption of the rust, the mass transfer of the electrolyte, the promotion of the cathodic reaction in rust and localization of the cathode site are future subjects.

The specimen was kept at 40%RH for 45 hours, then the point where potential was less noble in the filiform shape rust tip was seen. This potential was less noble than the other rust part, and then the part was less noble for three hours. The filiform shaped rust of a tip part grew along with the time process in this place. Therefore, the potential became less noble at the part of rusting, and the

place where the dissolution reaction of the iron produced could be limited as for the growth part of the rust. If the part of less noble potential can be found, prediction can be done the growth point of the rust, and the growth direction of rusting.

3.2 The pH distribution of the low alloy steels under atmospheric corrosion environment

The surface morphology where pure iron and ferritic alloys of the rust were eliminated after the corrosion cycle test was shown in Fig. 5. The corrosion morphology of pure iron and Fe-Ni ferritic alloy was general corrosion. On the other hand, in the case of Fe-Cr alloy, pitting corrosion was produced on the surface under the rust. Although the rusting formation shape of all the steels was the same as the filiform corrosion type, the surface condition of the Fe-Cr alloy was different from the iron and Fe-Ni alloy. Both Cr and Ni addition also had the effect

Fig. 5. Optical micrograph of the corroded surface of the iron and the ferritic alloy after elimination of the rust.

on the decreasing the corrosion rate in the atmospheric corrosion environment

Fig. 6 shows the pH distribution of the corroded surface on the low alloy steels after 30 min and 2 hours. The pH distribution on the Fe-Ni low alloy steel was spread for the homogeneity in all the area after 2 hours. In the case of Fe-Cr low alloy steel, after 2 hours the heterogeneous pH distribution was appeared in this figure. As the surface pH profile became heterogeneous, the corrosion on the Fe-Cr alloys under the atmospheric corrosion environment progresses for the heterogeneity. Therefore, the corrosion morphology shown in Fig. 5 was caused by the pH localization with the dissolution of alloy elements. It can be explained by the hydrolysis equilibrium as it can be known in the case of the stainless steel. As Fe and Ni anodic dissolution did not make the pH decline, the corrosion of iron and the Fe-Ni alloy were general corrosion. When the anodic dissolution of Cr was carried out, it is easy to decline pH and severe condition was achieved at the local site. And then the steel contained Cr was produced localized corrosion.

4. Conclusions

1) Rust grew up around the droplet circumference department, and it was found out that corrosion morphology was a micro filiform as for that form.

2) It was found out that rust growth is facilitated rapidly above 40% relative humidity under the artificial sea water and the $MgCl_2$ droplet adherence conditions, and is attributed in the $MgCl_2$ solution environment of the high concentration.

3) The small addition of Cr and Ni as the contained amount of alloy element was effective on decreasing of the corrosion rate in atmospheric corrosion environment. It can be found out by using SCHEM that the corrosion behavior on the Fe-Cr alloy was localized corrosion behavior.

4) The small addition of Cr and Ni as the contained amount of alloy element was effective on decreasing of the corrosion rate in atmospheric corrosion environment. It can be found out by using SCHEM that the corrosion behavior on the Fe-Cr alloy was localized corrosion behavior.

References

1. M. Stratmann, Corros. Sci., 27, 869 (1987).
2. M. Stratmann and H. Streckel, Corros. Sci.,30, 681 (1990).
3. M. Stratmann and H. Streckel, Corros. Sci., 30, 697 (1990).

Fig. 6. The pH distribution of the low alloy steel(Fe-3mass%Ni, Fe-3mass%Cr) at 30min and 1h during corrosion test.

4. M. Stratmann, H. Streckel, K. T. Kim, and S. Crockett, *Corros. Sci.*, **30**, 715 (1990).
5. S. Yee, R. A. Oriani, and M. Stratmann, *J. Electrochem. Soc.*, **138**, 55 (1991).
6. K. Honda, A. Usami, and H. Usami, *Zairyo-to-Kankyo*, **47**, 403 (1998).
7. K. Noda, M. Itou, A. Nishikata, and T. Tsuru, *Zairyo-to-Kankyo*, **47**, 396 (1998).
8. A. Tahara and T. Kodama, *Zairyo-to-Kankyo*, **47**, 391 (1998).
9. J. Wang and T. Tsuru, *Proc. 13th Int. Corros. Cong.* 1996, **4**, 344 (1996).
10. M. Yamashita, T. Doi, and H. Nagano, *Zairyo-to-Kankyo*, **47**, 384 (1998).
11. A. Usami, T. Inoue, and K. Tanabe, *Zairyo-to-Kankyo*,

12. K. Noda, H. Masuda, and T. Kodama, *Proc. 14th Int. Corros. Cong.* 1999, (1999).
13. H. Masuda, *Bulletin Iron and Steel Institute Japan*, **3**, 884 (1998).
14. R. C. Engstrom, S. Ghaffari, and H.Qu, *Anal. Chem.*, **64**, 2525 (1992).
15. B. R. Horrocks, M. V. Mirkin, D. T. Pierce, and A. J. Bard, *Anal. Chem.*, **65**, 1213 (1993).
16. H. Kim, M. Hayashi, K. Nakatani, N. Kitamura, K. Sasaki, J. Hotta, and H. Masuhara, *Anal. Chem.*, **68**, 409 (1996).
17. H. Kaneko, *J. Surface Finishing Soc. Japan*, **44**, 715 (1993).

47, 406 (1998).